Polymer Journal (2017) 49, 255–262

www.nature.com/pj

ORIGINAL ARTICLE

SPR study for analysis of a water-soluble glycopolymer interface and molecular recognition properties

Yuhei Terada[1], Hirokazu Seto[1], Yu Hoshino[1], Tatsuya Murakami[2], Shuhei Shinohara[3], Kaoru Tamada[4] and Yoshiko Miura[1]

Glycopolymers consisting of mannose and acrylamide with different mannose incorporation ratios (10 and 100%) were synthesized by reversible addition fragmentation chain transfer (RAFT) polymerization, and the polymer layers were prepared on a gold substrate. The detailed polymer layer structure and molecular recognition properties were analyzed by the surface plasmon resonance (SPR) technique. The glycopolymers formed pancake-like thin layers with thicknesses of ~2 nm in air and were swollen in the aqueous solution. The molecular recognition against concanavalin A (ConA) was also analyzed by SPR. Binding constants between glycopolymers and ConA were large enough to suggest multivalent effects. Binding rate constants of ConA to glycopolymers were in the same order; however, the dissociation rate constant was lower in the glycopolymer with a mannose ratio of 100% because of the high local mannose density near the binding point of ConA.
Polymer Journal (2017) **49,** 255–262; doi:10.1038/pj.2016.99; published online 19 October 2016

INTRODUCTION

Sugar–protein interactions are relevant to various biological phenomena such as cellular adherence, viral and toxin infections and metastasis of cancer.[1] Although sugars bind to proteins specifically, the interaction between a monovalent sugar and a protein is weak, with a binding constant of $K_a = 10^3$–$10^4\ M^{-1}$.[2–4] These weak interactions can be amplified by multivalent sugar assemblies and compounds such as glycolipid rafts, dendritic saccharides of glycoproteins and polysaccharides of glycosaminoglycans and mucins. This strong interaction of multivalent sugars is known as the 'cluster effect'.[5,6] Sugar binding proteins (lectins) have plural sugar binding sites, and the multivalent sugars could bind to the multiple sugar binding sites with an enhanced interaction.[7] The multivalent sugar compounds also amplify the sugar binding modes and the protein binding possibilities. The cluster effect is the amplification effect of these complex interactions.[8] It has been reported that artificial multivalent sugar compounds such as glycopeptides, clycodextrin derivatives and liposomes exhibit these cluster effects. Among them, polymers with pendant sugars have been developed and extensively studied because of the cluster effects and applicability for biomaterials.[9] By preparing sugar monomers, glycopolymers with different types of sugars or different sugar incorporation ratios could be easily designed via radical polymerization. Various types of glycopolymers have been synthesized,[8–12] and their strong and specific recognition of proteins have been reported.[13–16] As the glycopolymers show brilliant interaction toward proteins, they are promising for molecular recognition materials.

The glycopolymer interface can provide the function of molecular recognition. The glycopolymer-immobilized interfaces have been reported as biomaterials.[17–20] Considering the progress of proteomes and glycomics, the exhaustive analysis of sugar–protein interactions is becoming attractive. The glycopolymer-immobilized interface could provide an array for the analysis with an amplified affinity against protein. So far, we have reported a glycopolymer showing a specific affinity for proteins and viruses; however, the high-throughput analysis will be more important. To attain the high-throughput analysis with glycopolymers, the structure and the orientation of the glycopolymer are important considerations. Hence, analyzing the polymer layer on the material's surface and evaluating the correlation of the polymer structure with its binding ability to the target molecule is necessary. The relationship between the protein binding kinetics and the glycopolymer architecture especially carries weight. Analysis of the polymer layer, especially the analysis of the water-soluble polymer layer, is difficult. The water-soluble polymers have different polymer architecture in solvents because of various conditions such as the grafting method, the grafting density, the side chain and the temperature.[21–24]

For the analysis of the polymer-immobilized interface, surface plasmon resonance (SPR) is attractive.[25–27] SPR is one of the most sensitive methods used to detect the refractive index change on the surface of metal substrates. It is well known that the adsorption and

[1]Department of Chemical Engineering, Graduate School of Engineering, Kyushu University, Fukuoka, Japan; [2]Center for Nano Materials and Technology, Japan Advanced Institute of Science and Technology, Nomi, Ishikawa, Japan; [3]Department of Chemistry, Graduate School of Science, Kyushu University, Fukuoka, Japan and [4]Institute for Materials Chemistry and Engineering, Kyushu University, Fukuoka, Japan
Correspondence: Professor Y Miura, Department of Chemical Engineering, Graduate School of Engineering, Kyushu University, 744 Motooka, Nishi-ku, Fukuoka 819-0395, Japan.
E-mail: miuray@chem-eng.kyushu-u.ac.jp
Received 13 June 2016; revised 23 August 2016; accepted 25 August 2016; published online 19 October 2016

the desorption kinetics of biomolecules onto the metal surface can be measured using SPR techniques.[28,29] In addition, the thickness of the polymer layer on the metal surface can also be measured in nm scale. The SPR measurement can be performed not only in air and water but also in organic solvents. The refractive index of the polymer layer on the metal surface can be determined by a shift in the SPR spectrum. Furthermore, highly sensitized and exhaustive analysis of a number of biomolecular interactions is possible using two-dimensional SPR imaging techniques.[30–32]

Our group has reported a glycopolymer-immobilized interface for the development of biointerfaces and biosensors.[33–36] Although we have shown the molecular recognition of the glycopolymer interface, the detailed structure of the glycopolymer interface has not been clarified. In this study, we investigated glycopolymers carrying mannose with two different sugar incorporation ratios. The glycopolymers were synthesized via a reversible addition-fragmentation chain transfer (RAFT) polymerization, and thus thiol-terminated glycopolymers with controlled molecular weight and low polydispersity were obtained. Immobilization of the glycopolymers onto the gold substrate was confirmed using X-ray photoelectron spectroscopy (XPS). The refractive index and the thickness of the glycopolymer layer on the gold substrate in dry and wet conditions were estimated using SPR techniques. The binding of proteins onto the glycopolymer layer was also analyzed by kinetic measurements using SPR. It is important to analyze the correlation between the glycopolymer structure in the polymer-immobilized interface and the molecular recognition properties, especially when applying a screening method like SPR imaging to analyze various types of glycopolymers designed via radical polymerization. The polymer orientation and molecular recognition ability of the glycopolymer layers evaluated in this research are important in exhaustive designing of molecular recognition interfaces and for high-throughput analysis using water-soluble glycopolymers.

EXPERIMENTAL PROCEDURE

Materials

The following reagents were purchased from commercial sources and were used as received. Sodium methoxide (NaOMe), methanol (MeOH), acetone, ethanol (EtOH), chloroform ($CHCl_3$), toluene, hexane, calcium chloride ($CaCl_2$) and magnesium chloride hexahydrate ($MgCl_2{\cdot}6H_2O$) were obtained from Wako Pure Chemical Industries Ltd. (Osaka, Japan); sodium chloride (NaCl), *N,N*-dimethyl acetamide (DMAc), *N,N*-dimethyl sulfoxide deuteride (DMSO-d_6), sodium borohydride ($NaBH_4$) and heavy water (D_2O) were obtained from Kanto Chemical Co., Ltd (Tokyo, Japan); concanavalin A (ConA) was obtained from J-Oil Mills Inc. (Tokyo, Japan); glycine was obtained from Kishida Chemical Co., Ltd (Osaka, Japan). Acrylamide (AAm) and 2,2'-azobis isobutyronitrile (AIBN) (Wako Pure Chemical Industries Ltd) were recrystallized using $CHCl_3$ and acetone-MeOH before use, respectively.

Measurements

Proton nuclear magnetic resonance (^{1}H-NMR) measurements were performed using JEOL-ECP400 (JEOL Co., Tokyo, Japan) with DMSO-d_6 or D_2O as the solvent. Multiangle light scattering (MALS; Wyatt Technology Co., Santa Barbara, CA, USA) was used to measure the molecular weight of the glycopolymers. XPS (AXIS-ultra; Shimazu/Kratos, Kyoto, Japan) was used for the surface analysis of the glycopolymer-immobilized gold substrate. The water was purified using a Direct-Q Ultrapure Water System (Merck, Ltd, Darmstadt, Germany). The reflected light of the helium–neon laser ($\lambda = 632.8$ nm) irradiated onto the gold substrate was detected using a UV-1800 spectrometer (Shimazu, Kyoto, Japan) in all SPR measurements.

Synthesis of thiol-terminated glycopolymers

p-Acrylamidophenyl-2,3,4,6-*tetra*-*O*-acetyl-α-D-mannopyranoside (AcMan) and S-2-cyano-2-propyl S'-butyl trithiocarbonate (CPBTC) were synthesized according to the previous study (Scheme 1).[33,35] A mixture of AcMan and AAm (total monomer concentration: 2.0 mmol), 2.0 μmol of the RAFT reagent (CPBTC) and 8.0 μmol of AIBN were dissolved in 2.0 ml of DMAc and placed in a Pyrex tube. The feed ratios are summarized in Table 1 (**ManP10** and **ManP100**). The solution was degassed by three freeze–thaw cycles and sealed under vacuum, and the tube was incubated in a thermostatic oil bath at 70 °C for 20 h. DMAc was removed by vacuum concentration using an evaporator. Synthesized glycopolymers were stirred in MeOH and deacetylated by the addition of NaOMe at pH 10 for 1 h. MeOH was removed by vacuum concentration, and the residue was dissolved in MilliQ (Direct-Q, Merck Ltd.). $NaBH_4$ was added and stirred for 1 h to reduce the glycopolymers. The solution was dialyzed in MilliQ using a dialysis membrane with molecular weight cutoff of 1000 for 2 days (MilliQ was exchanged three times each day). The remained solution was freeze dried for over 24 h. The molecular weights of the glycopolymers were determined using MALS. The immobilization of the glycopolymers on the gold substrates was confirmed using XPS.

SPR measurements

In all experiments, the gold substrates were prepared by deposition of gold (50 nm) onto LaSFN9 (R-DEC Co., Ltd, Ibaraki, Japan) glass substrates using a vacuum evaporation method. All of the SPR measurements were performed in the Kretschmann configuration.[37] A 45° LasFN9 prism was used in all measurements. The SPR cell was made of Teflon and is resistant to organic solvents. A *p*-polarized helium–neon laser ($\lambda = 632.8$ nm) was used as the light source, and the reflected light at the interface was detected using a photodiode

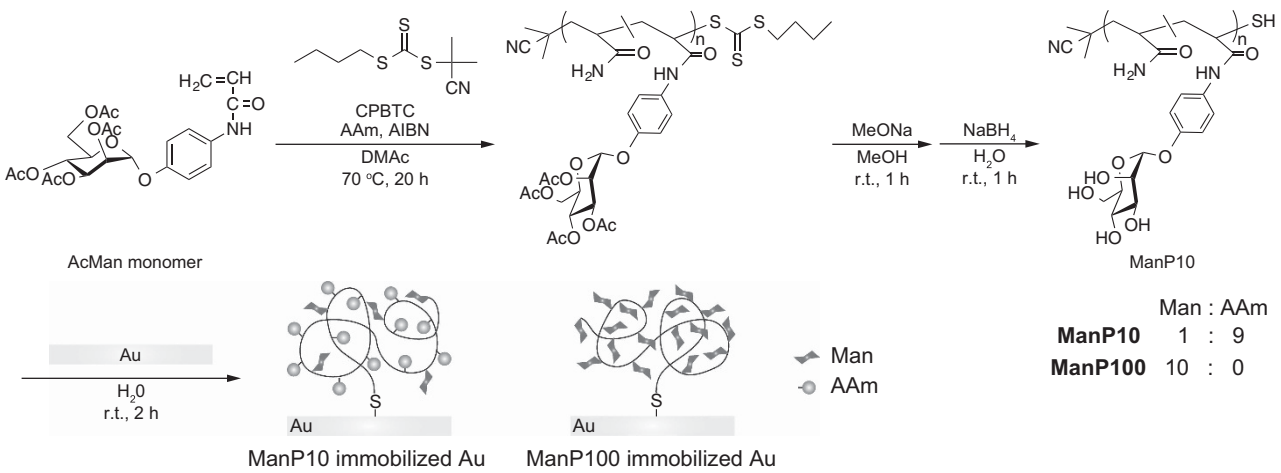

Scheme 1 Synthesis of thiol-terminated glycopolymers. A full color version of this figure is available at *Polymer Journal* online.

Table 1 Synthesis of thiol-terminated glycopolymers

Polymer	*Feed 1: AAm*	*Man ratio*[a] *(%)*	*Theoretical M_n ($\times10^{-4}$)*	*M_w SEC ($\times10^{-4}$)*	*M_w MALS ($\times10^{-4}$)*	*PDI*[b]	*Yield (%)*
ManP10	1:9	9.0	1.00	1.18	1.32	1.03	59
ManP100	10:0	100	3.30	0.17	3.38	1.03	49

Abbreviations: AAm, acrylamide; MALS, multiangle light scattering; Man, mannose; PDI, polydispersity index; SEC, size-exclusion chromatography.
[a]Man-incorporated ratio of the glycopolymers was calculated by comparing the total methylene proton of the main chain (1.0–2.5 p.p.m.) with the benzene ring proton signal (6.5–7.5 p.p.m.).
[b]PDI of the polymers was determined by MALS.

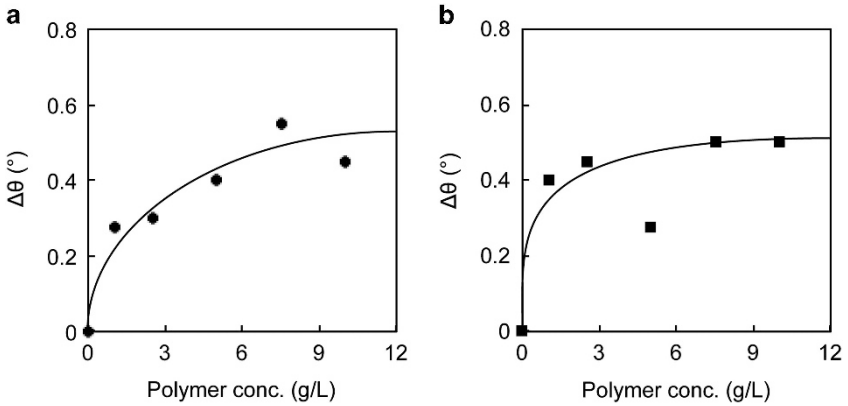

Figure 1 Surface plasmon resonance (SPR) angle shifts by immobilization of (**a**) **ManP10** and (**b**) **ManP100** onto gold substrate.

detector. The reflectivity of the light was measured as a function of the incidence angle (angle scan) and as a function of the time at a fixed incidence angle (kinetic scan).

Measurement of glycopolymer immobilization onto gold substrate using an SPR technique

A glycopolymer solution (solvent: MilliQ, glycopolymer concentration: 1.0–10 g l^{-1}) was injected into the SPR cell and incubated for 2 h, and a kinetic scan was performed at an incident angle of 55.5° during this process. MilliQ was injected to remove the remaining glycopolymers and incubated for 30 min. The angle scan was performed before and after the immobilization of glycopolymers to determine the refractive index of the glycopolymer layer.

Characterization of glycopolymer layer

Glycopolymers were immobilized on a gold substrate by injecting a 10 g l^{-1} glycopolymer aqueous solution and incubating for 2 h. MilliQ was injected to remove the remaining glycopolymers and incubated for 30 min. The angle scan was performed in various solvents to estimate the refractive index of the glycopolymers. The solvents were changed in order of water, acetone, ethanol, $CHCl_3$, toluene and hexane. The angle scan was also performed in air after drying the gold substrate using an N_2 blow. The thickness of the glycopolymer layer at the assumed refractive index of the layer was estimated by curve fitting the angle scan data in water and under dry conditions (air).

Analysis of protein binding onto a glycopolymer using SPR

Glycopolymers were immobilized on a gold substrate by injecting a 10 g l^{-1} glycopolymer aqueous solution and incubating for 2 h. MilliQ was injected to remove the remaining glycopolymers and incubated for 30 min. The solvent was exchanged to PBS(+) (pH 7.4, 137 mM NaCl, 2.68 mM KCl, 1.80 mM $CaCl_2$ and 0.49 mM $MgCl_2$) and ConA/PBS(+) (ConA concentration: 10–250 mM) was injected. A kinetic scan at an incident angle of 55.5° was performed during this process.

RESULTS AND DISCUSSION

Synthesis of glycopolymers

The glycopolymer polymerization results are summarized in Table 1. The sugar incorporating ratio (Man ratio) calculated from ^{1}H-NMR data was 9.0% and 100% in **ManP10** and **ManP100**, respectively. The Man ratio by ^{1}H-NMR was almost the same as the feed ratio. Both glycopolymers were 100-mer designed, and the molecular weights of the glycopolymers obtained by MALS were almost the same as the theoretical values. The polydispersity was small in both of the glycopolymers ($M_w/M_n < 1.1$), indicating that the RAFT living radical polymerization was performed successfully.

Although the molecular weight of **ManP100** by MALS matches that of the theoretical value, the molecular weight by size-exclusion chromatography varied drastically (1700) compared with the theoretical value (Supplementary Figure S2 in Supplementary Information). It indicated that conformation of **ManP100** is unique and has a folded structure with a much smaller inertia radius in aqueous solution. It is considered that this is because of the amphiphilicity and the intermolecular interactions of **ManP100** in aqueous solution. The conformation of **ManP100** is under investigation.

Immobilization of glycopolymers onto the gold substrate

The SPR angle (the angle of minimum reflectivity in angle scan data) shift to a higher angle ($\Delta\theta$) by immobilization of the glycopolymers onto a gold substrate in water is shown in Figure 1. The $\Delta\theta$ increased as the concentration of the glycopolymers increased in both polymers. The immobilization of the glycopolymers onto the gold substrate was saturated at 7.5 g l^{-1} in both polymers according to the SPR angle shift to the higher angle. The XPS spectra of the gold substrates are shown in Figures 2 and 3. In the C(1s) spectra of the unmodified gold substrate, peaks corresponding to C-H and C-C bonds (285.0 eV) (these peaks are due to residual dust), C-O bonds (286.2 eV) and C=O bonds (289.1 eV) were observed (Figure 2a). In the C(1s) spectra of the **ManP10**-immobilized gold substrate, peaks corresponding to C-H and C-C bonds (285.1 eV), C-O and C-S bonds (285.9 eV), C-N bonds (287.0 eV) and C=O bonds (289.8 eV) were observed (Figure 2b). In the C(1s) spectra of the **ManP100**-immobilized gold substrate, peaks corresponding to C-H and C-C

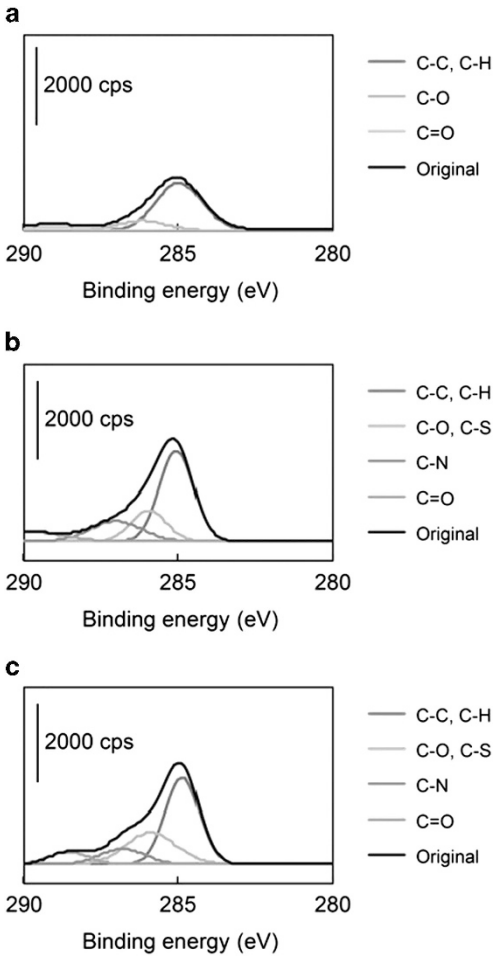

Figure 2 X-ray photoelectron spectroscopy (XPS) C(1s) spectrum of (**a**) unmodified, (**b**) **ManP10**-immobilized and (**c**) **ManP100**-immobilized gold substrate. A full color version of this figure is available at *Polymer Journal* online.

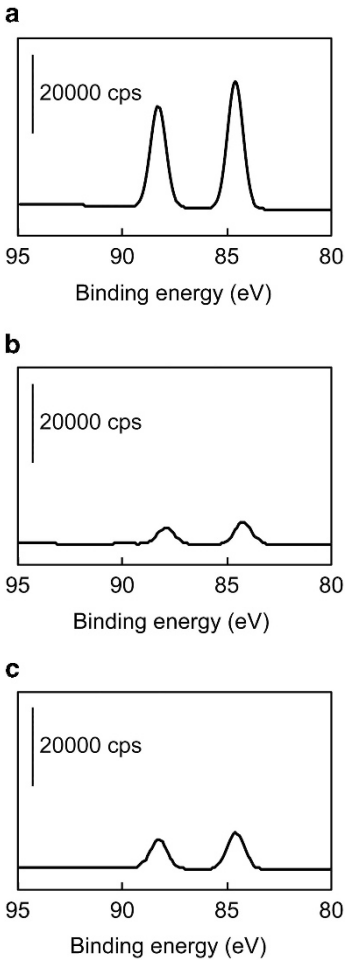

Figure 3 X-ray photoelectron spectroscopy (XPS) Au(4f) spectrum of (**a**) unmodified, (**b**) **ManP10**-immobilized and (**c**) **ManP100**-immobilized gold substrate.

bonds (284.9 eV), C-O and C-S bonds (285.9 eV), C-N bonds (286.8 eV) and C=O bonds (288.6 eV) were observed. In the Au (4f) spectra, two peaks corresponding to Au were observed in all gold substrates (Figure 3). The peak intensities of Au(4f) in the **ManP10**- and the **ManP100**-immobilized gold substrates were 17% and 28% of the unmodified substrate, respectively.

The adsorption of the glycopolymers onto the gold substrates was assumed as Langmuir binding, and hence the binding of each polymer was independent. In addition, it is suggested that the glycopolymers were uniformly immobilized onto the gold substrate.[38] The XPS spectra in the C(1s) suggested the immobilization of **ManP10** and **ManP100**. As a reference, the spectrum of the unmodified gold substrate was measured. The peak in C(1s) of the unmodified substrate was observed because of the residual dust that was much smaller than that of the glycopolymer substrate. The peak corresponding to the C-N and C-S bond was observed only in glycopolymers of **ManP10**- and **ManP100**-immobilized substrates. The increase in the peak intensity of the C(1s) and the decrease of the Au(4f) spectra indicated that glycopolymers were immobilized onto the gold substrate successfully. Comparing the Au(4f) spectra of the **ManP10**- and the **ManP100**-immobilized substrates, the peak intensity was ~1.7 times stronger in the **ManP100** substrate than in the **ManP10** substrate.[39] The peak intensity in C(1s) was almost the same. The amount of C in the polymer is 3.7 times stronger in **ManP100** compared with **ManP10**. Therefore, the C(1s) peaks also suggested the amount of bound polymer was larger in **ManP10**- than that in the **ManP100**-immobilized gold substrate.

Characterization of the glycopolymer layer using an SPR contrast variation technique

The angle at the minimum SPR reflective intensity (SPR angle) shifts due to the immobilization of **ManP10** and the SPR angle scan data in various solvents are shown in Figure 4 (the data of **ManP100** is shown in the Supplementary Information). The dashed line and the solid line represent the SPR reflection spectrum before (bare gold substrate) and after the immobilization of the glycopolymers, respectively. The SPR angles before and after the immobilization of the glycopolymers were compared. The SPR angle shifted to a higher angle in water ($n=1.333$), acetone ($n=1.357$), EtOH ($n=1.360$), hexane ($n=1.376$) and $CHCl_3$ ($n=1.441$), indicating that the refractive index of the glycopolymer layer is higher than that of the solvents. The SPR angle shifted to lower angle in toluene ($n=1.492$), indicating that the refractive index of the glycopolymer layer is lower than that of the solvents. The SPR angle shifts measured in these solvents indicate that

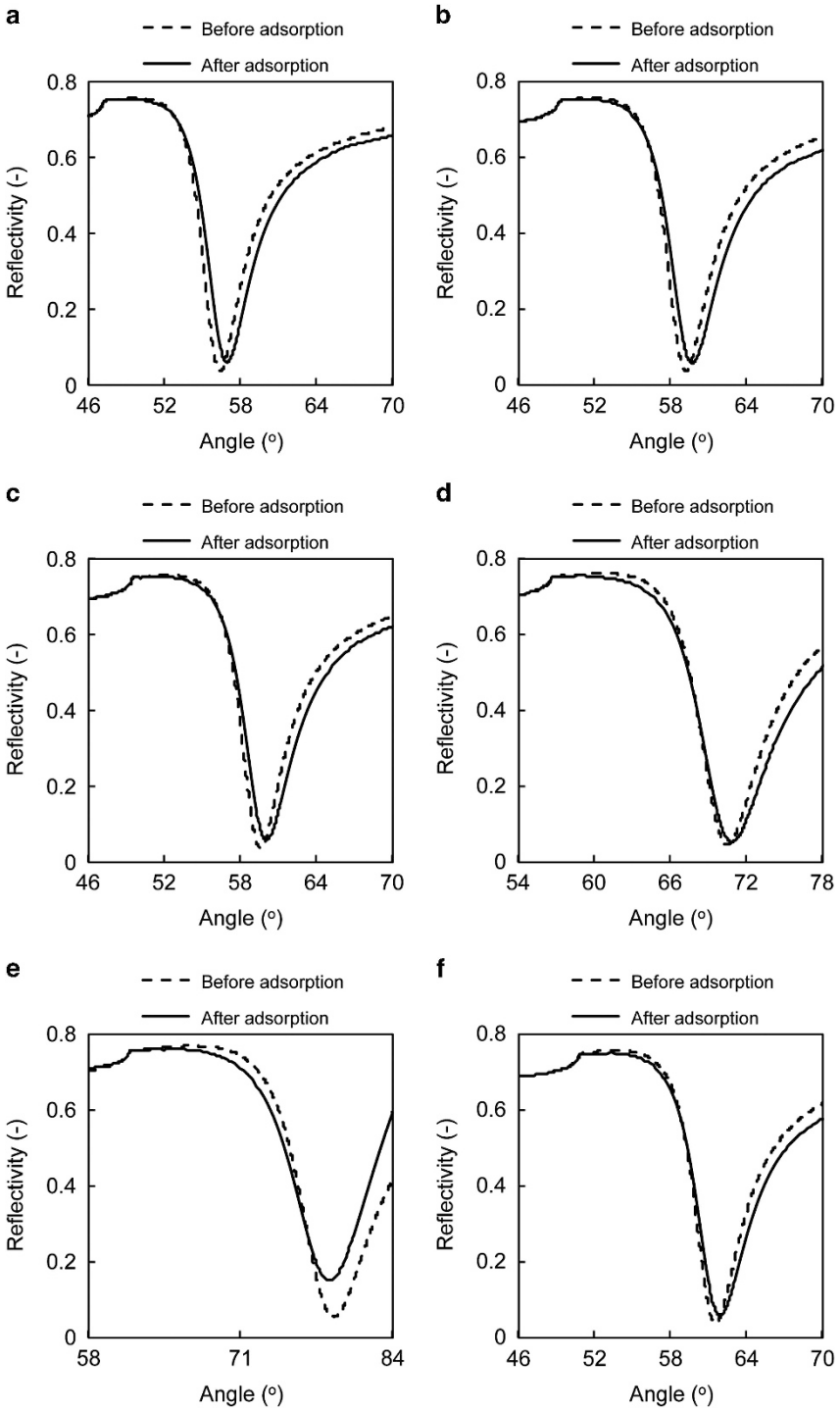

Figure 4 Surface plasmon resonance (SPR) curves of the unmodified and **ManP10**-immobilized gold substrate in (**a**) water, (**b**) acetone, (**c**) ethanol (EtOH), (**d**) chloroform ($CHCl_3$), (**e**) toluene and (**f**) hexane.

the refractive index of the glycopolymer layer (n_{GP}) is in range of $1.441 < n_{GP} < 1.492$.

The estimated thickness of the glycopolymer in water and in air is shown in Figure 5 as a function of the assumed refractive index.[40,41] According to the SPR angle scan data, the glycopolymer layers in water were estimated to be thicker than those in air. When the refractive index of the glycopolymer layer is in the range of $1.441 < n_{GP} < 1.492$, the thickness of the glycopolymer was ~ 2.2 nm in air without a solvent. The refractive index of the glycopolymer layer in water will be lower than that in the air because water molecules are involved in the glycopolymer layer, and the glycopolymer does not swell in air. Hence, the average refractive index of the glycopolymer layer is lower than 1.492. In both polymers, the layer in water is thicker than that in air. The estimated thickness from SPR suggested that the glycopolymer layer is swollen in aqueous solution to form the hydrophilic polymer layer.

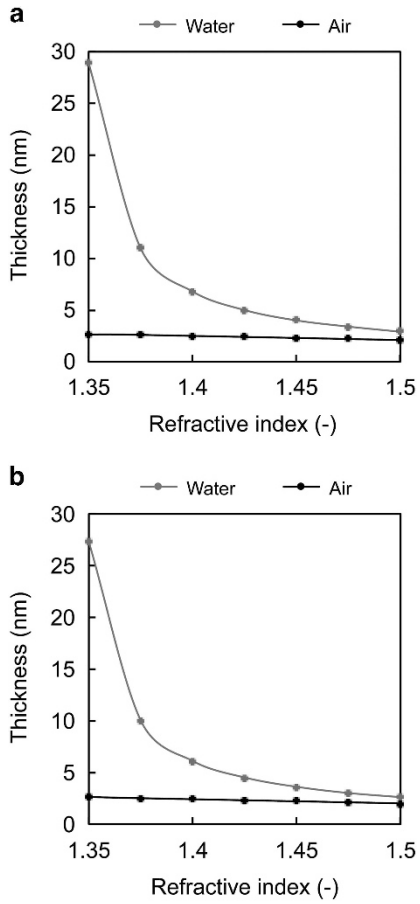

Figure 5 (**a**) **ManP10** and (**b**) **ManP100** layer thickness estimated from surface plasmon resonance (SPR) measurement. A full color version of this figure is available at *Polymer Journal* online.

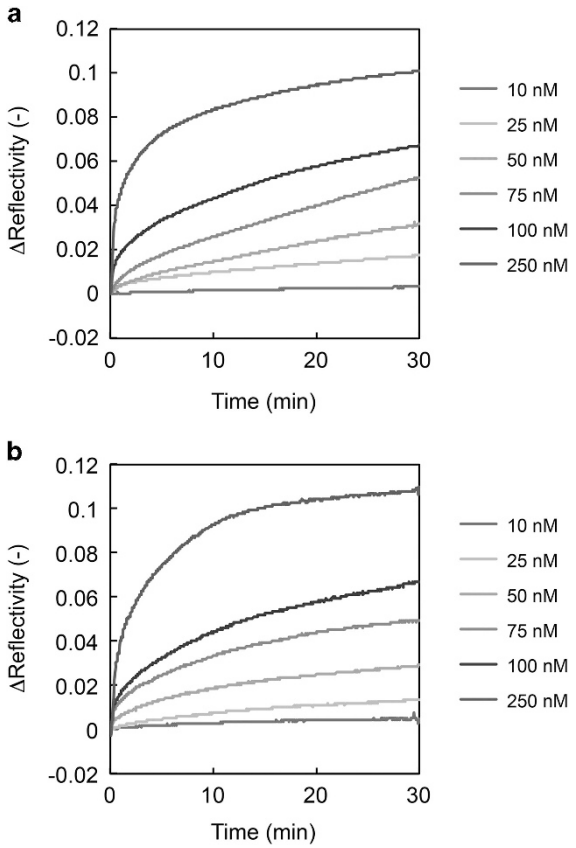

Figure 6 Surface plasmon resonance (SPR) reflectivity change by adsorption of concanavalin A (ConA) onto (**a**) the **ManP10**-immobilized and (**b**) the **ManP100**-immobilized gold substrate. A full color version of this figure is available at *Polymer Journal* online.

When we assume the average refractive index of the **ManP10** layer and **ManP100** layer to be the same, the polymer layer in water is thicker in **ManP10** than in **ManP100**. To be exact, considering the average refractive index of the glycopolymer layer of 1.35–1.45, the thicknesses of **ManP10** and **ManP100** are in the ranges of 4.0–29.0 and 3.6–27.3 nm, respectively. When we estimated the refractive index was 1.45 in reference to the polyacrylamide,[42] the thicknesses of the **ManP10** and **ManP100** layers were ~4.0 and 3.6 nm, respectively. Hence, it is indicated that the thickness of the polymer layer is about the same. However, we propose that the thickness of the polymer layer of **ManP10** is higher because **ManP10** contains more water in the polymer layer and is swollen, and **ManP100** has a folded structure as suggested from size-exclusion chromatography and MALS results.

The lengths of the polymers were calculated in the stretched model and the Flory model[43] that were ~30 and 12 nm, respectively. If the polymer was oriented vertically in the form of a polymer brush, the glycopolymers were more than 10 nm thick. The obtained thickness of ~2 nm in air suggested a pancake-like polymer layer formation because of the high surface free energy and a flexible polymer structure. In terms of polymer thin layers, 'pancake' structure is typical in grafting to method that has a two-dimensional thin layer with low density.[44] Genzer and colleagues[21] reported the change in the polyacrylamide brush layer height as a function of polymer grafting density. Consulting this and length of the glycopolymers, we considered that the height of the **ManP10** layer is approximately <7 nm in the assumed average refractive index of 1.35–1.45. The thicknesses of the **ManP100** and **ManP10** layers were almost the same in air because of the collapsed structure.

Table 2 Kinetic constants calculated from surface plasmon resonance (SPR) kinetic measurement

Polymer	k_{on} (10^3 M^{-1} s^{-1})	k_{off} (10^{-3} s^{-1})	K_a (10^7 M^{-1})
ManP10	13	1.1	1.2
ManP100	21	0.3	7.8

Considering the XPS results, the polymer density in **ManP10** was higher than that in **ManP100**. In addition, the thickness estimation of SPR suggested that **ManP10** formed a thicker layer than **ManP100** on the assumption of the same refractive index. The molecular weight of **ManP100** in size-exclusion chromatography was much smaller than that in MALS, suggesting the folded structure. However, the molecular weight of **ManP100** in size-exclusion chromatography and MALS was almost the same, suggesting the swollen structure. The thicker layer of **ManP10** was considered to be affected by the conformation of glycopolymers. A difference of density and the thickness of the polymer layer was considered to reflect the conformation in the water solution.

Analysis of protein binding onto glycopolymer using SPR technique

The SPR reflectivity change by adsorption of ConA onto the glycopolymer-immobilized gold substrate is shown in Figure 6.

The data fitting was performed by the single exponential curve shown in Equation (1), and the binding/dissociation rate constants (k_{on} and k_{off}) were calculated by binding relaxation method.

$$\Delta R = \Delta R_{max}\left(1 - e^{-\frac{t}{\tau}}\right) \quad (1)$$

$$\text{where} \quad \tau^{-1} = k_{on}[ConA] + k_{off} \quad (2)$$

Here, ΔR and ΔR_{max} are the SPR reflectivity change and the reflectivity change at the point of binding saturation, respectively. The reciprocal of the relaxation time (τ) obtained from each data was plotted against the ConA concentration (Supplementary Figure S6 in Supplementary Information). The apparent k_{on} and k_{off} were obtained as the slope and intercept of the y axis of the linear correlations (Table 2). The binding constant K_a was also calculated from the fraction of k_{on} and k_{off}.

The binding constants for **ManP10** and **ManP100** were 1.2×10^7 and 7.8×10^7 (M^{-1}), respectively. The binding constants of **ManP10** and **ManP100** were in the same order and that of **ManP100** was ~6 times that of **ManP10**. The binding rate constants of the glycopolymers were also in the same order, and the rate constants of **ManP100** was about double of **ManP10**. The dissociation rate constants of **ManP100** was <30% of **ManP10**.

The binding constants of both polymers were much larger than the binding constants of monovalent mannose to ConA (10^3–10^4 M^{-1}).[2] The large binding constants indicate both polymers exerted the cluster effects, and the polymers bound to ConA in bivalent modes by the cluster effects. Considering the primary sequence of two polymers, the local mannose density of **ManP100** is 10 times higher than that of **ManP10**. However, the amount of polymer bound of **ManP10** is larger than that of **ManP100** according to the XPS results. Therefore, the mannose density in two dimensions is similar in both polymer layers that results in the binding constants and the binding rate constants with the same order. As **ManP100** has a higher local sugar density than **ManP10**, the binding constant of **ManP100** was higher than that of **ManP10**. In addition, we considered ConA bound to the periphery of polymer layer based on the thicknesses and the protein size. The size of ConA is ~9 nm, and each mannose binding point is 6.5 nm.[45] The polymer layer is thinner than or nearly the same size as ConA.

The binding rate constant of **ManP100** was approximately twice as large as that of **ManP10** and was in the same order, and little difference was suggested. However, the dissociation rate constant showed the large difference that reflected to the binding constants. As mentioned above, **ManP100** was considered to have higher local sugar density than the **ManP10** layer that was advantageous to the high association rate and the less dissociation rate constants. Mori *et al.*[46] reported a detailed study of a two-dimensional mannose cluster and its binding kinetics. They reported the multiple interaction and the local sugar densities were important in the interaction between ConA and mannose. They reported the remarkable decrease of k_{off} by increasing the sugar density, and this was the same in our results. This indicates that the difference in the dissociation rate constants has reflected a higher binding constant of **ManP100**.

Both glycopolymers were affected by multiple interactions and showed the binding constants because of the two-dimensional sugar cluster, but the binding kinetic was much affected by the local sugar density. In addition, because the natural ligand of ConA is trimeric mannose, one sugar binding site is fitted to the dense sugar cluster like **ManP100**.[47] There is a possibility that the interaction affected the change of binding mode in **ManP100** and **ManP10**.

These results suggested the importance of the sugar cluster effect in sugar–protein interactions and that the sugar density is important in binding constants and kinetics. A higher sugar density strongly affected the decreasing rate constants and the increasing binding constants. Our results suggest that the sugar–protein interaction with the glycopolymer was not affected by the orientation of the glycopolymer. The sugar–protein interaction showed a multivalent effect based on the primary polymer sequence (sugar ratio in the polymer). These results suggested the glycopolymer layer was suitable for analysis of glycomics. The high-throughput analysis of the sugar–protein interaction is under investigation in our group.

CONCLUSION

In this report, we prepared a glycopolymer interface via RAFT living radical polymerization and investigated the detailed structure and molecular recognition by an SPR technique. Two glycopolymers with different sugar ratios formed a thin layer via an Au-S bond. The density of the glycopolymer with the lower sugar ratio was higher on the substrate. The glycopolymer formed a pancake-like thin (2 nm) layer and swelled in aqueous solution. The density and thickness of the glycopolymer were thought to be related to the polymer structure in water. The sugar recognition protein of ConA strongly interacted with the glycopolymer-immobilized interface because of the multivalent effects. The binding constants and the kinetics were affected by the glycopolymer density. In particular, the local sugar density on the glycopolymer contributed to the high binding constants and the decrease of the dissociation rate constants. We believe this detailed study of the glycopolymer layer could provide vital information regarding sugar–protein interactions and have critical impacts in areas, including various diseases and infections.

CONFLICT OF INTEREST

These authors declare no conflict of interest.

ACKNOWLEDGEMENTS

The MALS measurements and discussion were supported by Professor Atushi Maruyama and Dr Naohiko Shimada (Tokyo Institute of Technology). This work was supported by a Grant-in-Aid for Scientific Research B (15H03818), a Grant-in-Aid for Exploratory Research (16K14007) and a Grant-in-Aid for Scientific Research on Innovative Areas (16H01036).

1 Taylor, M. E. & Drickamer, K. *Introduction to Glycobiology* (Oxford University Press, Oxford, UK, 2002).
2 Mandal, D. K., Kishore, N. & Brewer, C. F. Thermodynamics of lectin-carbohydrate interactions. Titration microcalorimetry measurements of the binding of N-linked carbohydrates and ovalbumin to concanavalin A. *Biochemistry* **33**, 1149–1156 (1994).
3 Dam, T. K. & Brewer, C. F. Thermodynamic studies of lectin-carbohydrate interactions by isothermal titration calorimetry. *Chem. Rev.* **102**, 387–430 (2002).
4 Murrey, H. E. & Hsieh-Wilson, L. C. The chemical neurobiology of carbohydrates. *Chem. Rev.* **108**, 1708–1731 (2008).
5 Lee, Y. C. & Lee, R. T. Carbohydrate-protein interactions: basis of glycobiology. *Acc. Chem. Res.* **28**, 321–327 (1995).
6 Mammen, M., Choi, S.-K. & Whitesides, G. M. Polyvalent interactions in biological systems: implications for design and use of multivalent ligands and inhibitors. *Angew. Chem., Int. Ed.* **37**, 2754–2794 (1998).
7 Schnaar, R. L. & Lee, Y. C. Polyacrylamide gels copolymerized with active esters. New medium for affinity systems. *Biochemistry* **14**, 1535–1541 (1975).
8 Miura, Y., Hoshino, Y. & Seto, H. Glycopolymer nanobiotechnology. *Chem. Rev.* **116**, 1673–1692 (2016).
9 Bernard, J., Hao, X., Davis, T. P., Barner-Kowollik, C. & Stenzel, M. H. Synthesis of various glycopolymer architectures via RAFT polymerization: from block copolymers to stars. *Biomacromolecules* **7**, 232–238 (2006).
10 Fernandez-Megia, E., Correa, J., Rodríguez, I. & Riguera, R. A click approach to unprotected glycodendrimers. *Macromolecules* **39**, 2113–2120 (2006).

11 Ghadban, A. & Albertin, L. Synthesis of glycopolymer architectures by reversible-deactivation radical polymerization. *Polymers* **5**, 431–526 (2013).
12 Chen, Y., Espeel, P., Reinicke, S., Du Prez, F. E. & Stenzel, M. H. Control of glycopolymer nanoparticle morphology by a one-pot, double modification procedure using thiolactones. *Macromol. Rapid Commun.* **35**, 1128–1134 (2014).
13 Ting, S. R. S., Chen, G. & Stenzel, M. H. Synthesis of glycopolymers and their multivalent recognitions with lectins. *Polym. Chem.* **1**, 1392–1412 (2010).
14 Zhang, Q., Collins, J., Anastasaki, A., Wallis, R., Mitchell, D. A., Becer, C. R. & Haddleton, D. M. Sequence-controlled multi-block glycopolymers to inhibit DC-SIGN-gp120 binding. *Angew. Chem.* **52**, 4435–4439 (2013).
15 Gou, Y., Geng, J., Richards, S.-J., Burns, J., Becer, C. R. & Haddleton, D. M. A detailed study on understanding glycopolymer library and ConA interactions. *J. Polym. Sci. A Polym. Chem.* **51**, 2588–2597 (2013).
16 Yilmaz, G. & Becer, C. R. Precision glycopolymers and their interactions with lectins. *Eur. Polym. J.* **49**, 3046–3051 (2013).
17 Yang, Q., Xu, Z.-K., Dai, Z.-W., Wang, J.-L. & Ulbricht, M. Surface modification of polypropylene microporous membranes with a novel glycopolymer. *Chem. Mater.* **17**, 3050–3058 (2005).
18 Mateescu, A., Ye, J., Narain, R. & Vamvasaki, M. Synthesis and characterization of novel glycosurfaces by ATRP. *Soft Matter* **5**, 1621–1629 (2009).
19 Yang, Q., Kaul, C. & Ulbricht, M. Anti-nonspecific protein adsorption properties of biomimetic glycocalyx-like glycopolymer layers: effects of glycopolymer chain density and protein size. *Langmuir* **26**, 5746–5752 (2010).
20 Park, H., Rosencrantz, R. R., Elling, L. & Böker, A. Glycopolymer brushes for specific lectin binding by controlled multivalent presentation of N-acetyllactosamine glycan oligomers. *Macromol. Rapid Commun.* **36**, 45–54 (2015).
21 Wu, T., Efimenko, K. & Genzer, J. Combinatorial study of the mushroom-to-brush crossover in surface anchored polyacrylamide. *J. Am. Chem. Soc.* **124**, 9394–9395 (2002).
22 Balamurugan, S., Mendez, S., Balamurugan, S. S., O'Brien, M. J. II & López, G. P. Thermal response of poly(N-isopropylacrylamide) brushes probed by surface plasmon resonance. *Langmuir* **19**, 2545–2549 (2003).
23 Gunkel, G., Weinhart, M., Becherer, T., Haag, R. & Huck, W. T. S. Effect of polymer brush architecture on antibiofouling properties. *Biomacromolecules* **12**, 4169–4172 (2011).
24 Bousquet, A., Awada, H., Hiorns, R. C., Dagron-Lartigau, C. & Billon, L. Conjugated-polymer grafting on inorganic and organic substrates: a new trend in organic electronic materials. *Prog. Polym. Sci.* **39**, 1847–1877 (2014).
25 Stuart, M. A. C., Huck, W. T., Genzer, J., Müller, M., Ober, C., Stamm, M., Sukhorukov, G. B., Szleifer, I., Tsukruk, V. V. & Urban, M. Emerging applications of stimuli-responsive polymer materials. *Nat. Mater.* **9**, 101–113 (2010).
26 Lee, B. S., Chi, Y. S., Lee, K.-B., Kim, Y.-G. & Choi, I. S. Functionalization of poly(oligo(ethylene glycol) methacrylate) films on gold and Si/SiO_2 for immobilization of proteins and cells: SPR and QCM studies. *Biomacromolecules* **8**, 3922–3929 (2007).
27 Kambhampati, D. K., Jakob, T. A., Robertson, J. W., Cai, M., Pemberton, J. E. & Knoll, W. Novel silicon dioxide sol-gel films for potential sensor applications: a surface plasmon resonance study. *Langmuir* **17**, 1169–1175 (2001).
28 Liedberg, B., Nylander, C. & Lundström, I. Surface plasmon resonance for gas detection and biosensing. *Sensors Actuat.* **4**, 299–304 (1983).
29 Mrksich, M., Sigal, G. B. & Whitesides, G. M. Surface plasmon resonance permits in situ measurement of protein adsorption on self-assembled monolayers of alkanethiolates on gold. *Langmuir* **11**, 4383–4385 (1995).
30 Lee, H. J., Goodrich, T. T. & Corn, R. M. SPR imaging measurements of 1-D and 2-D DNA microarrays from microfluidic channels on gold thin films. *Anal. Chem.* **73**, 5525–5531 (2001).
31 Bassil, N., Maillart, E., Canva, M., Lévy, Y., Millot, M.-C., Pissard, S., Narwa, R. & Goosens, M. One hundred spots parallel monitoring of DNA interactions by SPR imaging of polymer-functionalized surface applied to the detection of cystic fibrosis mutations. *Sensors Actuat. B* **94**, 313–323 (2003).
32 Wolf, L. K., Fullenkamp, D. E. & Georgiadis, R. M. Quantitative angle-resolved SPR imaging of DNA-DNA and DNA-drug kinetics. *J. Am. Chem. Soc.* **127**, 17453–17459 (2005).
33 Takara, M., Toyoshima, M., Seto, H., Hoshino, Y. & Miura, Y. Polymer-modified gold nanoparticles via RAFT polymerization: a detailed study for a biosensing application. *Polym. Chem.* **5**, 931–939 (2014).
34 Toyoshima, M., Oura, T., Fukuda, T., Matsumoto, E. & Miura, Y. Biological specific recognition of glycopolymer-modified interfaces by RAFT living radical polymerization. *Polym. J.* **42**, 172–178 (2010).
35 Terada, Y., Hashimoto, W., Endo, T., Seto, H., Murakami, T., Hisamoto, H., Hoshino, Y. & Miura, Y. Signal amplified two-dimensional photonic crystal biosensor immobilized with glycol-nanoparticles. *J. Mater. Chem. B* **2**, 3324–3332 (2014).
36 Seto, H., Takara, M., Yamashita, C., Murakami, T., Hasegawa, T., Hoshino, Y. & Miura, Y. Surface modification of siliceous materials using maleimidation and various functional polymers synthesized by reversible addition-fragmentation chain transfer polymerization. *ACS Appl. Mater. Interfaces* **4**, 5125–5133 (2012).
37 Kretschmann, E. & Raether, H. Z. Notizen: radiative decay of non radiative surface plasmons excited by light. *Z. Naturforsch. A* **23**, 2135–2136 (1968).
38 Jordan, C. E. & Corn, R. M. Surface plasmon resonance imaging measurements of electrostatic biopolymer adsorption onto chemically modified gold surfaces. *Anal. Chem.* **69**, 1449–1456 (1997).
39 Bramblett, A. L., Boeckl, M. S., Hauch, K. D., Ratner, B. D., Sasaki, T. & Rogers, J. Determination of surface coverage for tetraphenylporphyrin monolayers using ultraviolet visible absorption and x-ray photoelectron spectroscopies. *Surf. Interface Anal.* **33**, 506–515 (2002).
40 Yokota, Y., Miyazaki, A., Fukui, K.-I., Enoki, T., Tamada, K. & Hara, M. Dynamic and collective electrochemical responses of tetrathiafulvalene derivative self-assembled monolayers. *J. Phys. Chem. B* **110**, 20401–20408 (2006).
41 Tamada, K., Ishida, T., Knoll, W., Fukushima, H., Colorado, R. Jr, Graupe, M., Shmakova, O. E. & Lee, T. R. Molecular packing of semifluorinated alkanethiol self-assembled monolayers on gold: influence of alkyl spacer length. *Langmuir* **17**, 1913–1921 (2001).
42 Franklin, J. & Wang, Z. Y. Refractive index matching: a general method for enhancing the optical clarity of a hydrogel matrix. *Chem. Mater.* **14**, 4487–4489 (2002).
43 Rubinstein, M. *Polymer Physics* (Oxford Univ. Press, NY, 2003).
44 Advincula, R. C., Brittain, W. J., Caster, K. C. & Rühe, J. *Polymer Brushes* (WILEY-VCH Verlag GmbH & Co. KGaA, Weinheim ISBN, 2004).
45 Jack, A., Weinzierl, J. & Kalb, A. J. An X-ray crystallographic study of demetallized concanavalin A. *J. Mol. Biol.* **58**, 389–395 (1971).
46 Mori, T., Toyoda, M., Ohtsuka, T. & Okahata, Y. Kinetic analyses for bindings of concanavalin A to dispersed and condensed mannose surfaces on a quartz crystal microbalance. *Anal. Biochem.* **395**, 211–216 (2009).
47 Loris, R., Maes, D., Poortmans, F., Wyns, L. & Bouckaert, J. A structure of the complex between concanavalin A and methyl-3,6-di-O-(alpha-D-mannopyranosyl)-alpha-D-mannopyranoside reveals two binding modes. *J. Biol. Chem.* **271**, 30614–30618 (1996).

Supplementary Information accompanies the paper on Polymer Journal website (http://www.nature.com/pj)